

## **Study of a Magnetic Photocatalyst Based on Hemin with Axial Ligand and its Degradation under Visible Light**

**Liu, X. Y., Zhang, X. N. and Li, N.X.\***

School of Chemistry& Chemical Engineering, Tianjin University of Technology,  
Tianjin,300384, P.R. China

Received 22 Aug. 2014;

Revised 5 Nov. 2014;

Accepted 6 Nov. 2014

**ABSTRACT:** An investigation was conducted on hemin modified with axial ligand loaded onto magnetic carriers which created a kind of visible-light activated photocatalyst with good magnetic property. This photocatalyst exhibits excellent photo-degradation performance and can be readily reclaimed in the degradation of bis-phenol A (BPA) in aqueous solution under visible light. The catalysts were characterized by thermal gravimetric analysis (TG), transmission electron microscopy (TEM), magnetometer (VSM) and IR spectra. The effects of different operation parameters on the photocatalytic reaction have also been investigated. The highest degradation ratio reached up to 94.75% after 6 hours under optimized operation conditions. Moreover, the photocatalysts could be readily reclaimed by magnetic separation with an external magnetic field and when it was reused for 5 times under the same conditions, the degradation ratio of BPA solution during the last time was still higher than 90%. Possible mechanism on BPA degradation was also investigated based on a series of control experiments. The main intermediate of BPA degradation was monitored by GC/MS analysis.

**Key words:** Photo-degradation, Metalloporphyrin, Bis-phenol A

### **INTRODUCTION**

The widespread disposal of industrial waste-water containing organic compounds has led to serious contamination in many countries worldwide. Weathering of organic compounds through oxidation, hydrolysis, or other chemical reactions occurring in the wastewater phase can produce toxic metabolites (Bianco, Prevot *et al.*, 2001; Neppolian *et al.*, 2002; Pagga & Brown, 1986). Adsorption and coagulation practices are effective ways to treat wastewater, which always result in secondary pollution. Consequently, a more promising technology based on advanced oxidation process (AOP) has been studied and heterogeneous photocatalytic oxidation process developed as one of the AOP (Fang *et al.*, 2009).

Photocatalysis using semiconductor catalysts such as TiO<sub>2</sub> is widely used for removing organic compounds from water. The photocatalytic efficiency of TiO<sub>2</sub> to degrade organic compounds depends on photo-induced electrons and holes produced when irradiated under ultraviolet (UV) light (Bertelli & Selli, 2006; Braghetta, 1995). It means TiO<sub>2</sub> can only work as photocatalyst under UV light. Therefore, study of the visible light-driven photocatalyst has been a major focus in the research field of photocatalysis.

Porphyrin is one kind of the materials have the photo-electric conversion properties (Grandos *et al.*, 2009). Photo-induced electron transfer takes place on metalloporphyrins under illumination. The electrons transfer from the porphyrin ring (as the electron donor) to the central metal after being excited by photon. After the charge separated, the metalloporphyrins end up in oxidative and reductive electron-hole pairs just like a semiconductor, which gives metalloporphyrins the photocatalytic properties. The research for metalloporphyrins as visible light-activated photocatalysts for photocatalytic oxidation of organic pollutants has been reported (Hger *et al.*, 2001; She *et al.*, 2009; Rismayani *et al.*, 2004).

Hemin is nature iron porphyrin with high photo-absorption capacity. It can be extracted directly from animal blood to avoid the low yields of porphyrin synthesis. Due to its nature origin, good optical performance and easy to obtain, hemin is a good choice for heterogeneous photocatalytic material. However, the photo-absorption of hemin mainly at about 380nm, so in this study we intend to modify hemin to shift its absorption band to visible light region. The phenomenon that metalloporphyrins is

\*Corresponding author E-mail:linx68@sina.com

coordinated with axial ligands is very common especially for green-plant and photosynthetic bacteria, in which such co-ordinations show significant effects on both the primary charge separation in the reaction center and energy transfer in antenna systems (Deng *et al.*, 2003). The absorption band of metal porphyrin will get gearshift by introducing axial ligand to the central metal (Yang *et al.*, 2009). In our study, we chose pyridine and 2-methyl-imidazole as two kinds of ligands to modify hemin.

Another question for semiconductor catalysts such as  $\text{TiO}_2$  is separation from the treated water after each run. The traditional methods like sedimentation, centrifugation and filtration are time consuming and become increasingly inefficient as the particle size diminishes, as they are easy for smaller particles to stay suspended in the water, penetrate through filtration materials, and clog filter membranes (Bao *et al.*, 2004; Malato *et al.*, 2003). In order to solve the question mentioned above we anchor the porphyrins to a magnetic carrier. Due to the magnetic property, the catalyst can be easily separated from the treated water by an external magnetic field and when the external magnetic field being removed the catalyst recover highly dispersed. Another advantage of the immobilization is effectively reducing the self-reactions between porphyrin molecules which is an important factor affecting metalloporphyrin's photocatalytic efficiency (Knoer & Volger, 1994).

In this paper, we prepared a kind of visible light activated bio-mimetic catalyst with magnetic property and its photocatalytic properties were studied.

## MATERIALS & METHODS

Chemical materials and reagents: Hemin was supplied by Tianjin Institute of Life Sciences; cyanuric chloride was purchased from Tianjin crossed chemical Company. Other reagents used including Ferrous sulfate ( $\text{FeSO}_4 \cdot 7\text{H}_2\text{O}$ ), ferric chloride ( $\text{FeCl}_3 \cdot 6\text{H}_2\text{O}$ ), cellulose, BPA, 2-methylimidazole, pyridine, terephthalic quinone (BQ), silver nitrate, N,N-dimethyl formamide (DMF), and tert-butanol (TBA) were of analytical grade and bought from Tianjin Jiangtian unity Technology Company. The water used was double distilled water.

Synthesis of the magnetic carrier: According to the literature (Ma *et al.*, 2012; Ma *et al.*, 2012), we got nano  $\text{Fe}_3\text{O}_4$  prepared by using an ultrasound-assisted co-precipitation method. Then cellulose solution prepared according to reference (Mao *et al.*, 2006) was used to bear  $\text{Fe}_3\text{O}_4$  to make the magnetic carrier.

Modification of hemin: Modified hemin was prepared by mixing hemin and ligand with a molar ratio of 1:1 and string for 4 hours in solvent dimethylformamide. The differences between hemin and axial complexes were shown in the Fig. 1 while the discussion was placed in the chapter of Characterization. The UV-Vis spectra of the samples were obtained from a U-3900H UV-Vis (HITACHI Company in Japan). The FeP in the legend denotes hemin, in which P indicates the porphyrin part of hemin, and they are accepted in this article without other explains.

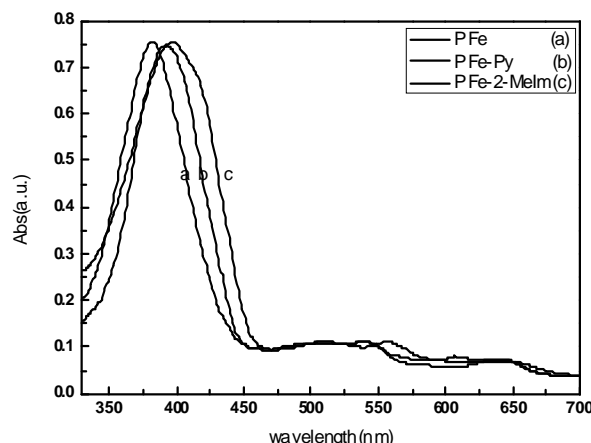


**Fig. 1. UV/ Vis spectra of Hemin and Modified Hemin**

Synthesis of Magnetic Photocatalyst: According to the literature (Yang *et al.*, 2014), cyanuric chloride was reacted with the magnetic carrier and modified hemin to make the modified hemin photocatalyst immobilized on the magnetic carrier.

Characterization of Photocatalyst: IR spectra were recorded with a infrared spectrometer (Bruker TENSOR27, Germany). The morphology of the sample was observed by using transmission electron microscopy (TEM) (Philips Tacnai G2F20, Netherlands). Thermal gravimetric analysis measurements were performed on a thermoanalyzer (TG) (Netzsch TG209F3, Germany), with a heating rate of  $10^\circ\text{C}\cdot\text{min}^{-1}$  under flowing  $\text{N}_2$  atmosphere. The hysteresis loop of the sample at 300 K was measured by a magnetometer (VSM) (MPMS-XL-7, Quantum Design, USA).

Photo-degradation experiments: The photocatalytic activities of the photocatalyst were evaluated by the degradation of the BPA solution under a 300 W Xe lamp illumination. This reaction was carried out in 50 mL glass beakers stirred on a magnetic stirrer. 50 mL of BPA solution (certain concentration) was added to make a desired substrate,

and then the reaction was initiated by the addition of the photocatalyst. Sample aliquots (5 mL) were withdrawn at regular time intervals from the reactor. The concentration of BPA in the filtered aqueous solution was determined by measuring the absorbance at 224 nm on a UV-Vis spectrophotometer. Prior to the measurement, a calibration curve was obtained by using the standard BPA solutions. The analysis of the intermediate during BPA degradation was performed by GC/MS (7890A GC system, 5975C inert XL MSD, Agilent Technologies, USA).

The degradation ratio of BPA was calculated by using the following formula:

$$\text{Degradation ratio} = [(C_0 - C_t) / C_0] \times 100\%$$

Where,  $C_0$  is the initial concentration of BPA and  $C_t$  is the concentration of BPA at a reaction time of t.

## RESULTS & DISCUSSIONS

UV-Vis spectroscopy provides a fast and valuable method for monitoring the differences of hemin and modified hemin. Fig. 1 (a) shows that the maximum absorption peak of hemin is at 382nm, which is in the ultraviolet region. When it is modified with pyridine (b) and 2-methylimidazole (c), the maximum absorption undergoes different levels of red shifts and the absorption peak widens too. Individually, the absorption band of 2-methyl-imidazole ligand complex shifts to 403 nm, which is greater than pyridine ligand's 397 nm.

These results can be explained by Gouterman four orbital model. The porphyrin molecule's Soret band is produced by the transition of  $a_{1u}(\pi)-e_g(\pi^*)$ , belonging to the  $\pi-\pi^*$  transitions' second electronic excited state of the porphyrin; pyridine derivatives are a class of five-membered heterocyclic aromatic compounds with two nitrogen atoms. Nitrogen atoms in the ring possess  $sp^2$  hybrid orbitals with lone electron pair, which can be used as a strong electron donor ligands to metal ions. When ligand and the hemin react, because of the introduction of strong nucleophilic objects, the charge of pyridine transfers to the porphyrin ring through  $Fe^{3+}$ , increasing the electronic density of the porphyrin ring, resulting in  $a_{1u}(\pi)$  orbital energy increasing and the energy gap to the  $e_g(\pi^*)$  decreasing, making Soret band red shift (Peng & Wang, 2012). So as to imidazole ligand.

In general, the factors affecting the coordination reaction are mainly electronic effect and steric effect. As the nucleophilic (basicity) of Pyridine and 2-methylimidazole incremented, from the viewpoint of the electronic effect, the stability of the complex is strengthened; and the steric hindrance caused by the electrophilic group at the ortho position of the N atom of 2 - methylimidazole

is weaker than its electronic effect. Therefore, 2-methyl imidazole using as a ligand can produce more pronounced red shift.

**Table 1. IR spectrum of the photocatalyst**

Frequency (cm <sup>-1</sup> )	Absorption	Function
1718	C=O stretching vibration	Carboxylic groups
1621-1399	porphyrin ring skeleton stretching vibrations	Porphurin ring
1138 and 1063	C-O stretching vibrations	Primary and tertiary alcohol of microcrystalline cellulose Red shifted by the macrocyclic aromatic conjugation system of porphyrin.
530	Fe <sup>3+</sup>	

The main features of IR spectrum of the photocatalyst are shown in the Tabel 1. It can be inferred from these data, porphyrin were successful loaded onto the magnetic carrier.

The thermal decomposition of the catalyst measured by thermo gravimetric analysis (TG) shows three consecutive mass losses in Fig. 2 (a). The weight loss under 120 ! (1.42%) could be attributed to the evaporation of adsorbed water on the catalyst. The main loss between 250~350 ! belongs to the metal porphyrin (21.78%) and the last 9.39% loss is cellulose. The mass of the materials remains unchanged until around 700.

Fig. 2 (b) shows the magnetic hysteresis loop of the sample at 300 K. The sample was para-magnetic with a saturation magnetization (Ms) of 35.563 emu/g. Therefore, the catalysts are able to be separated and collected on magnetic field.

The TEM image of the as-prepared catalyst, as shown in Fig. 3 (c), confirms that the samples is composed of spherical nano structures with a particle size of 10 nm. The core with dark color is magnetic carrier, while the shell outside in a light color is modified porphyrin.

When 50 mL aqueous solution of BPA (20 mg/L) was placed in the darkness for six hours the degradation ratio was below 10%, whether with photocatalyst or not. When it was placed under light, the degradation ratio was about 25% without the photocatalyst and if we added 7.5 mg photocatalyst in the solution of BPA, the degradation ratio was much higher. Detailed data is in the Fig. 3.

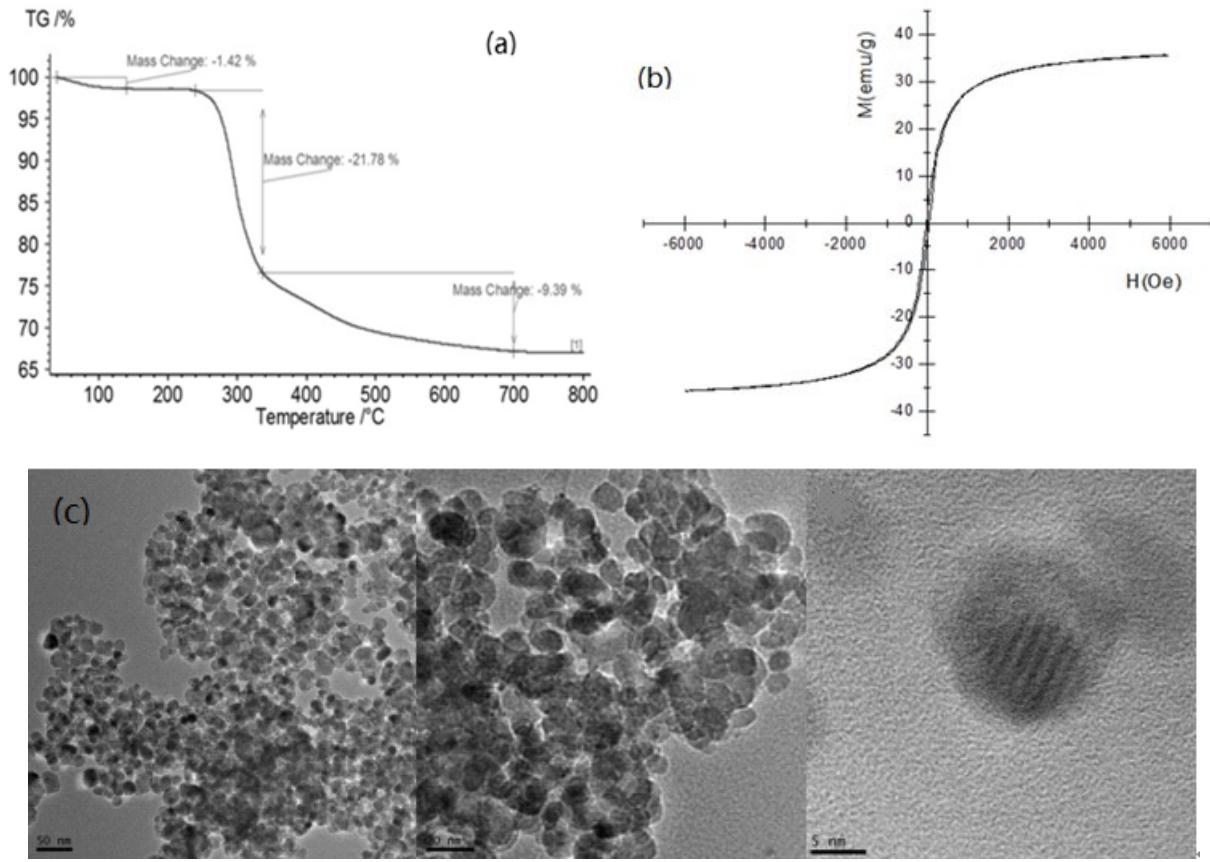


**Fig.2.** Thermo-gravimetric analysis (a), VSM analysis (b) and TEM images (c) of the photocatalyst, respectively

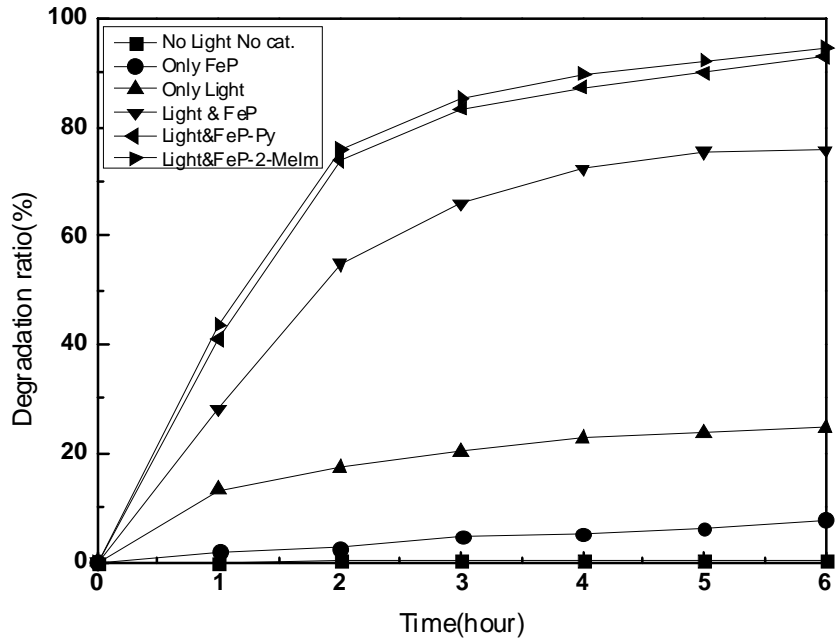


**Fig. 3.** Degradation of BPA in different systems

In the same degradation condition stated, different degradation effects, caused respectively by unmodified hemin catalyst and two kinds of modified hemin catalysts were compared. Modified hemin catalysts have higher degradation ratios than the unmodified one; hemin with 2-MeIm ligand works better than that with Py ligand. As mentioned above, the red shift of 2-Melm complexes appears greater, which means it is more effective to absorb visible light.

The degradation in different conditions were investigated (in Py-FeP for example) in order to figure out the impact of BPA concentrations, catalyst dose and pH of the solution onto the reaction.

In order to study the effect of BPA initial concentration on the degradation, a series of experiments were conducted with various initial concentration of BPA from 10 mg/L to 50 mg/L for 6

h. In these experiments, the BPA solution was at pH 7 and the dose of catalyst is 0.15 g/L. It is clearly to see in the Fig. 4 (a) that different concentrations of the substrate have consistent degradation trend, which increases fast at the first two hours and after that the reaction rate slows down and tends to balance at last. Among them, the degradation ratio is the highest (92.9%) when the concentration is 20 mg/L. Increasing concentration of BPA implies that more BPA molecules will be available to be removed by the same amount of active species generated. But when the concentrations of the substrate surpass a certain extent, because of the limited amount of the active species, part of BPA molecules might not be fully contacted with the active species, which makes the reaction rate decrease. Hence, the remaining experiments were performed with a BPA initial concentration of 20 mg/L.

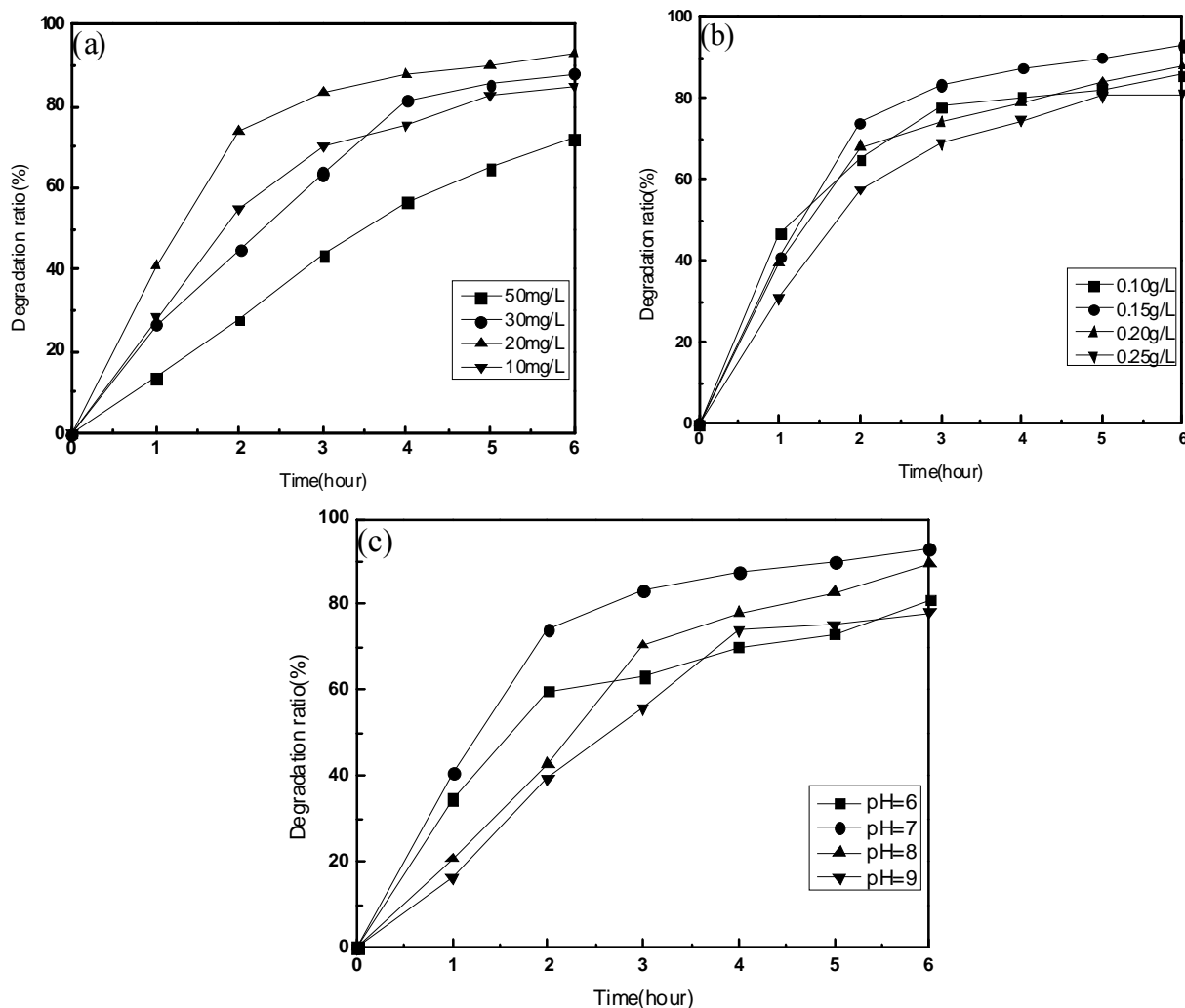


**Fig. 4. Effects of different reaction parameters on BPA degradation: (a) effect of initial concentration of BPA, (b) effect of the catalyst dose,(c) effect of pH**

Fig. 4 (b) shows as the concentration of BPA remains 20 mg/L and at pH 7, when catalyst dosage increases from 0.10 g/L to 0.15 g/L, the degradation ratio increases from 82.53% to 92.9 %. Given the amount of BPA in the reaction solution unchanged, with the increase of the dose of the catalyst, total active surface area increases, and hence active species increase (Gim'enez *et al.*, 1999). However, due to an increase of turbidity of the suspension with high dose of photocatalyst, there would be a decrease in penetration of light and hence the amount of photon to activate the catalyst decreases (Rideh *et al.*, 1997). Thus it could be concluded that higher dose of catalyst (such as 0.20 g/L and 0.25 g/L) might not be useful both in view of aggregation as well as reduced irradiation field due to light scattering.

To investigate the effect of pH on the ratio of photocatalytic degradation, the photo degradation of BPA (20 mg/L) in the presence of catalyst (0.15 g / L) under different pH (6-9) for 6h were conducted. The experimental results are shown in Fig. 4(c). It is evident that the degradation of BPA is pH-dependent. The maximum degradation (94.75%) is obtained at pH value 7. That value comes closest to the pH value of BPA solution itself. The degradation ratio declines when the pH value changes. One possible reason is that the original acid-base balance is destroyed by extra H<sup>+</sup> or OH<sup>-</sup> and inhibits the generation of free radicals. According to a previous report about the mechanism of photocatalytic degradation of organic pollutants (Zhang *et al.*, 2012), we added the hole-trapping agent (DMF), oxygen radical scavenger (BQ), hydroxyl radical scavenger (TBA) and electron capture agents (AgNO<sub>3</sub>) to clarify active ingredients in the degradation process. In these experiments, BPA solution was 20 mg/L and at pH 7. The dose of catalyst was 0.15 g/L and the capture agents were 1.5 g/L to bring them into full play.

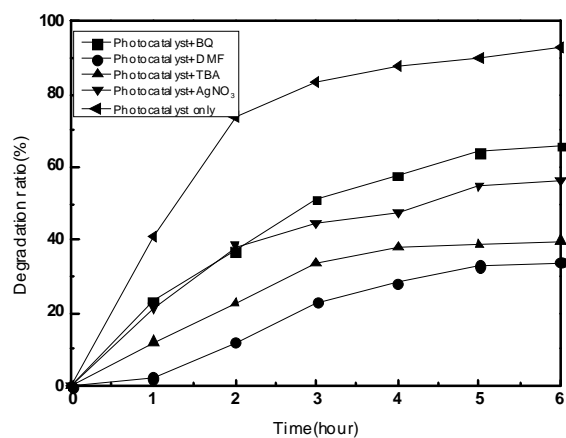


Fig. 5. Effects of BPA photo-degradation with different trapping agents

Conjecture can be made from curves seen from Fig. 5, compared with the degradation without trapping agents, all of the capture agents have obvious influence on the removal of BPA, but the addition of AgNO<sub>3</sub> has the most rapid depressing effect. That's due to the decrease of electrons would directly affect the generation of the free radicals which play an important role in the reaction of degradation. These phenomena indicate that electron hole pair and hydroxyl radicals are the primary active species responsible for the degradation of BPA.

This result is consistent with referred literature (Wang *et al.*, 2011), the metal porphyrins can produce electrons and holes when they are activated by light. Hydroxyl radicals and oxygen radicals are generated when photo-generated holes and light-generated electrons are captured by H<sub>2</sub>O molecules in the solution and O<sub>2</sub> molecules adsorbed on the catalyst.

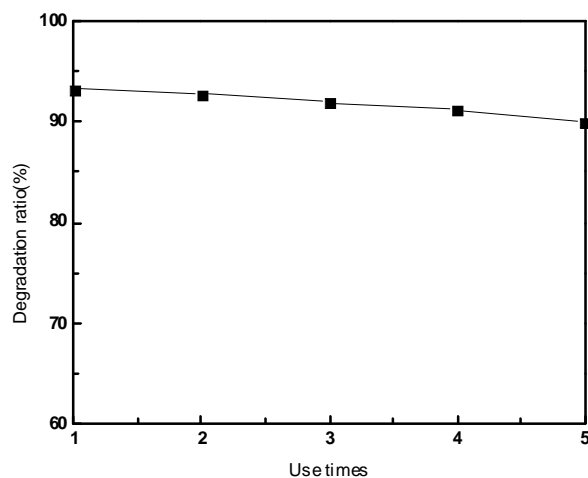
The intermediate products formed in the photocatalytic degradation process were monitored by GC-MS under the operation conditions reported previously (Tao *et al.*, 2009), and the results were shown in Table 2. Here we selected several possible materials known in the course of BPA's degradation.

Table 2. Intermediate products of BPA photocatalytic degradation

molecular formula	molecular weight(m/z)	molecular structure
C <sub>9</sub> H <sub>10</sub> O	134	
C <sub>6</sub> H <sub>6</sub> O	94	
C <sub>9</sub> H <sub>10</sub> O	134	
C <sub>4</sub> H <sub>10</sub> O	74	
C <sub>5</sub> H <sub>10</sub> O	86	

In the degradation process, we also keep track of the UV-Vis spectrum of BPA solution for six hours. Curves "a" to "g" in Fig. 6 are the ultraviolet absorptions of BPA from 0h to 6h, from which we can see absorbance value at characteristic absorption peaks of BPA (224 nm and 278 nm) are gradually reduced and the absorbances of the near-ultraviolet

region are also gradually reduced close to zero; there is no appearance of new absorption peaks in the entire degradation. Thus it can be inferred that BPA is gradually degraded to CO<sub>2</sub> and H<sub>2</sub>O without secondary contamination.



**Fig. 6. Recycling experiment in the photocatalytic degradation of BPA in the presence of photocatalyst under visible light**

The recycling property is an important indicator for the evaluation of catalyst's performance. Therefore, the catalyst was collected after used, and then washed and dried. Degradation experiment was repeated and the results in Fig. 7 showed BPA degradation ratio had a downward trend, but even in the fifth experiment, the degradation ratio was still more than 90%, which is ascribed to the fact that the self-reactions between FeP molecules is prevented when they are immobilized on the carrier.

## CONCLUSIONS

In this study, natural hemoglobin was chosen as raw materials in this experiment, and its ability to absorb visible light was improved through introducing axial ligands to the Fe<sup>3+</sup>. The modified metal porphyrin was loaded onto a magnetic carrier to prepare photocatalyst with good magnetic property. The photocatalytic activity of modified hemin photocatalyst was satisfactorily demonstrated by the degradation of bis-phenol A (BPA) in aqueous solution. This photocatalyst could be readily reclaimed by magnetic separation with an external magnetic field and still keeps high photocatalytic activity after being used for 5 rounds. The mechanism and main intermediate products of BPA degradation have also been investigated in this study. The development of porphyrin-based photo-catalysts

provides an alternative approach in utilizing solar visible light. And we believed that through continuous study, porphyrins would play a more important role in the photocatalytic degradation of organic matter.

## REFERENCES

- Bao, N., Feng, X., Yang, Z., Shen, L. and Lu, X. (2004). Highly efficient liquid-phase photo oxidation of an azo dye methyl orange over novel nanostructured porous titanate-based fiber of self-supported radially aligned H<sub>2</sub>Ti<sub>8</sub>O<sub>17</sub>·1.5H<sub>2</sub>O Nanorods. *Environment Science and Technology*, **38**, 2729–2736.
- Bertelli, M. and Selli, E. (2006). Reaction paths and efficiency of photocatalysis on TiO<sub>2</sub> and of H<sub>2</sub>O<sub>2</sub> photolysis in the degradation of 2-chlorophenol. *J. Hazardous Materials*, **138**, 46–52.
- Bianco-Prevot, A., Baiocchi, C., Brussino, M.C., Pramauro, E., Savarino, P., Augugliaro, V., Marci, G. and Palmisano, L. (2001). Photocatalytic degradation of acid blue 80 in aqueous solutions containing TiO<sub>2</sub> suspensions. *Environment Science & Technology*, **35**, 971–976.
- Braghetta, A. (1995). The influence of solution chemistry and operating conditions on nanofiltration of charged and uncharged organic macromolecules. Doctoral Dissertation, University of North Carolina, Chapel Hill, NC.
- Fang, H., Venkata, S. R. K., Madapusi, S., Dharmarajan, R. and Ravi, N. (2009). Tailored titanium dioxide photocatalysts for the degradation of organic dyes in wastewater treatment. *Applied Catalysis*, **359**, 25–40.
- Feng, J., Zhang, H. J., Xiang, J. F., Ai, X. Ch., Zhang, X. K., Xu, G. Z. and Zhang, J. P. (2003). Influence of axial coordination on the photophysical property of excited state of zinc porphyrin. *J. Science in China (Series B)*, **46**(2), 137–143.
- Gim'enez, J., Curc'o, D. and Queral, M. A. (1999). Photocatalytic Treatment of Phenol and 2,4-Dichlorophenol in a Solar Plant in the Way to Scalingup. *Catalysis Today*, **54**, 229–243.
- Grandos, O. G. and Ortega, F. M. (2009). Degradation of atrazine using metalloporphyrins supported on TiO<sub>2</sub> under visible light irradiation. *Catalysis Communications*, **11**(8), 727–731.
- Hger, M., Holmberg, K., Gonsalves, A. M. and Serra, A. C. (2001). On the mechanism of carboxilic acid co-catalyst assisted metalloporphyrin oxidations. *Colloids and Surfaces A-Physicochemical and Engineering Aspects*, **247**, 183–185.
- Knoer, G. and Vogler, A. (1994). Photochemistry and photophysics of antimony (III) hyper porphyrins: activation of dioxygen induced by a reactive excited state. *Inorganic Chemistry*, **33**(2), 314–318.
- Ma, Q. L., Dong, X. T., Wang, J.X., Liu, G. X. and Yu, W. S. (2012). Chemical preparation methods of ferriferrous oxide nanomaterials. *Chemical Industry and Engineering Progress*, **31**(3), 562–573.
- Ma, X. L., Shang, H. Zh., Zhao, Y. Q., Sun, X. R. and Zhang,

- X. M. (2012). Synthesis and surface modification of nanometer  $\text{Fe}_3\text{O}_4$ . *Fine and Specialty Chemicals*, **20(2)**, 26–31.
- Malato, S., Blanco, J., Campos, A., Ca'eres, J., Guillard, C., Herrmann, J. M. and Ferna'dez-Alba, A. R. (2003). Effect of operating parameters on the testing of new industrial titania catalysts at solar pilot plant scale. *Applied Catalysis B: Environmental*, **42**, 349.
- Mao, Y., Zhou, J. and Cai, J. (2006). Effects of coagulants on porous structure of membranes prepared from cellulose in NaOH urea aqueous solution. *J. Membrane Science*, **279**, 246.
- Nepolian, B., Choi, H. C., Sakthivel, S., Arabindoo, B. and Murugesan, V. (2002). Solar light induced and  $\text{TiO}_2$  assisted degradation of textile dye reactive blue 4. *Chemosphere*, **46**, 1173–1181.
- Pagga, U. and Brown, D. (1986). The degradation of dye, behavior of dyestuffs in aerobic biodegradation tests. *Chemosphere*, **15**, 479–491.
- Peng, Y. L. and Wang, Sh. J. (2012). Study on the spectroscopic properties of coordination reaction between Zn porphyrin and imidazoles derivatives. *Chemical Research and Application*, **24(2)**, 182–186.
- Rideh, L., Wehrer, A., Ronze, D. and Zoulalian, A. (1997). Photocatalytic degradation of 2-chlorophenol in  $\text{TiO}_2$  aqueous suspension: modeling of reaction ratio. *Industrial & Engineering Chemistry Research*, **36**, 4712–4718.
- Rismayani, S., Fukushima, M., Sawada, A., Ichikawa, H. and Tatsumi, K. J. (2004). Effects of peat humic acids on the catalytic oxidation of pentachlorophenol using metalloporphyrins and Metallophthalocyanines. *J. Molecular Catalysis A-Chemical*, **217**, 13–19.
- She, Y. B., Wang, W. J. and Li, G. J. (2012). Oxidation of p/o-cresols to p/o-hydroxy -benzaldehydes catalyzed by metalloporphyrins with molecular oxygen. *Chinese Journal of Chemical Engineering*, **20**, 262–266.
- Tao, H., Hao, S. Q. and Liu, J. (2009). Reaction mechanism of BPA photo-degradation by Ti-MCM-41 in aqueous solutions. *J. Water Resources & Water Engineering*, **20(4)**, 39–42.
- Wang, P., Luo, F. G., Cao, T. T., Rao, Z., Fang, Y. F. and Huang Y. P. (2011). Properties and photocatalytic mechanism of porphyrin and metal porphyrin. *J. China Three Gorges University (Natural Sciences)*, **33(5)**, 84–92.
- Yang, Y., Chen, H. and Jeong, Y. J. (2009). Nam enhanced reactivities of iron (IV)-oxo porphyrin p-cation radicals in oxygenation reactions by electron-donating axial ligands. *Chemistry-A European Journal*, **15(39)**, 1039–1046.
- Yang, Zh. H., Yan, Sh. X., Zhang, Z. Y. and Li, N. X. (2014). Photocatalytic detradation of bisphenol A in water using A visible light-activated biomimetic catalyst. *Fresenius Environmental Bulletin*, **23(2)**, 523–530.
- Zhang, Y. H., Zhang, N., Tang, Z. R. and Xu, Y. J. (2012). Graphene transforms wide band gap ZnS to a visible light photocatalyst. The new role of graphene as a macromolecular photosensitizer. *J. ACS. NANO*, **6**, 9777–9789.